Volume 57(8): 731–739, 2009
Journal of Histochemistry & Cytochemistry
http://www.jhc.org

ARTICLE

Esterified Cholesterol Is Highly Localized to Bruch's Membrane, as Revealed by Lipid Histochemistry in Wholemounts of Human Choroid

Martin Rudolf and Christine A. Curcio

Department of Ophthalmology, University of Alabama at Birmingham, Birmingham, Alabama (MR,CAC), and University Eye Hospital Lübeck, Universitätsklinikum Schleswig-Holstein, Lübeck, Germany (MR)

SUMMARY Accumulation of neutral lipids in Bruch's membrane (BrM) is a major age change in human retina and contributes to the formation of extracellular lesions associated with age-related macular degeneration. We developed a BrM–choroid wholemounting technique suitable for reliable staining and evaluated different fluorescent lipid dyes for topographic semiquantitative analysis of BrM lipids. Thin BrM–choroid complexes with partially stripped choroid from 10 aged donor eyes were prepared with an optimized wholemounting technique. Preparation quality was monitored by examining 1-μm-thick sections of representative samples. The staining patterns of Nile Red, BODIPY 493/503, filipin for unesterified cholesterol (UC-F), filipin for esterified cholesterol (EC-F), and Oil Red O in wholemounts were compared with their staining patterns in chorioretinal sections, using wide-field epi-fluorescence microscopy. Wholemounts exhibited optimal flatness on the BrM side. Reduced tissue thickness allowed reliable dye penetration and staining of BrM. Only EC-F was with high specificity localized to BrM and demonstrated an intense and distinct granular staining pattern not previously appreciated in chorioretinal sections. All other lipid dyes also stained choroidal or retinal tissue intensely. No dye provided perfect characteristics in regard to representing all neutral lipid classes present in BrM or to fluorescence intensity. Nevertheless, only EC-F was highly localized to BrM with a specific granular pattern. Because direct assays indicate that esterified cholesterol is abundantly present in BrM, we consider EC-F the most valuable choice for analyzing neutral lipid deposits in human BrM. **(J Histochem Cytochem 57:731–739, 2009)**

KEY WORDS
Bruch's membrane
wholemount
lipids
cholesterol
aging
age-related maculopathy

PHOTORECEPTORS IN THE HUMAN RETINA depend on the choroid, a remarkable vascular bed located behind them in the eye (Hogan 1972). Up to 1000 mm^2 in area and 200–300 μm in thickness, the choroid has the highest blood flow in the human body. Arteries enter from the sclera, ramify into a plexus, and form the choriocapillaris, a dense capillary bed. The metabolic supply of the outer third of the neurosensory retina, including photoreceptors, is exclusively provided by this plexus. The innermost 2–4 μm of the choriocapillaris is Bruch's membrane (BrM), a planar pentilaminar structure that functions as a specialized intima (Curcio et al. 2001). BrM is positioned between the choriocapillaris and the retinal pigment epithelium (RPE), a versatile cell layer dedicated to maintaining photoreceptor homeostasis. For instance, the RPE forms the outer blood–retina barrier, controls metabolite exchange between the choriocapillaris and photoreceptors, and phagocytizes and recycles photoreceptor outer segments. Extensions of BrM outward, between the individual lumens of the choriocapillaris, are called intercapillary pillars (Figure 1B). Unhindered translocation across BrM of nutrients to and metabolites from the RPE is essential for normal vision (Ethier et al. 2004).

With advanced age in normal eyes, BrM markedly accumulates neutral lipids that bind Oil Red O (Pauleikhoff et al. 1990; Curcio et al. 2001; Haimovici et al. 2001), a stain recognizing unesterified cholesterol (UC) and esterified cholesterol (EC), triglycerides, and free fatty acids (Adams and Bayliss 1975). This accumulation probably increases BrM hydraulic resistivity

Correspondence to: Martin Rudolf, MD, University Eye Hospital Lübeck, Universitätsklinikum Schleswig-Holstein, Ratzeburger Allee 160, 23538 Lübeck, Germany. E-mail: martin.rudolf@uk-sh.de
Received for publication December 30, 2008; accepted April 1, 2009 [DOI: 10.1369/jhc.2009.953448].

 0022-1554/09/$3.30

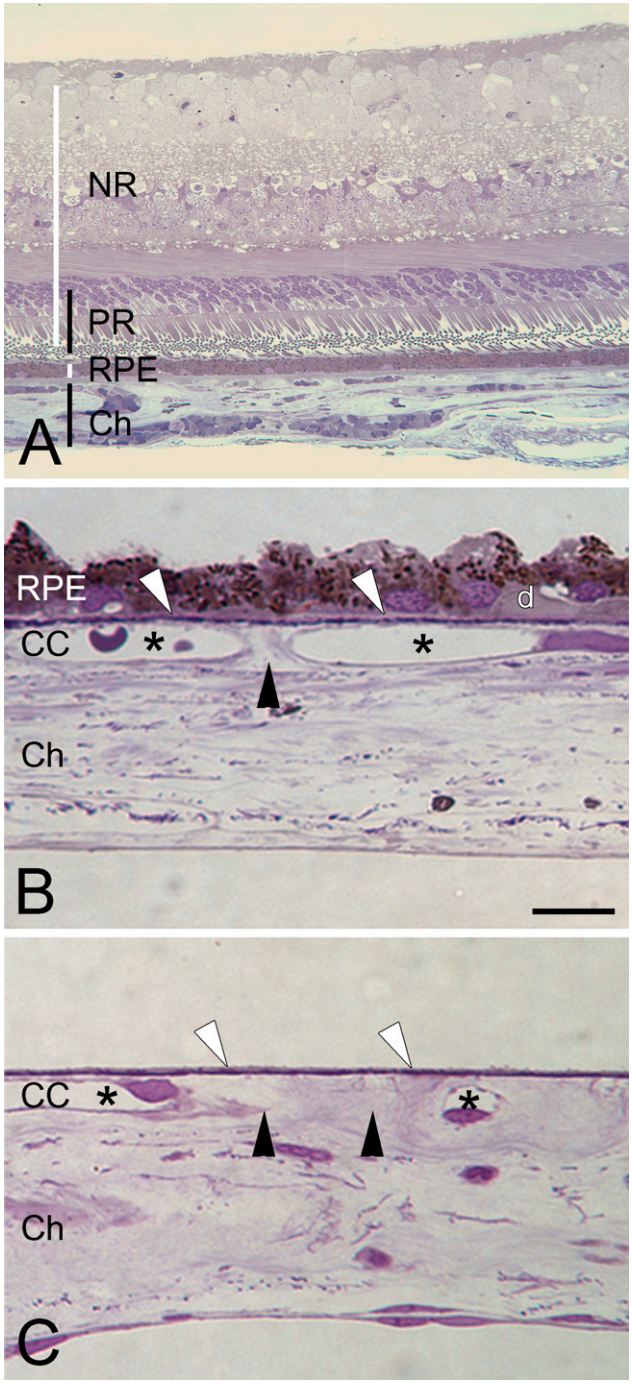

Figure 1 Chorioretinal anatomy and preparation quality of Bruch's membrane (BrM) wholemounts. (**A**) Ten-μm section of the posterior pole of an eye, stained with 1% toluidine-O blue. NR, neuroretina; PR, photoreceptors; RPE, retinal pigment epithelium; Ch, choroid. (**B,C**) Semi-thin sections of wholemount preparation, here from the macula. Panels show tissue after removal of the retina (top) and removal of large choroidal vessels and most connective tissue (bottom). CC, choriocapillaris. (**B**) RPE on, including sub-RPE debris and a very small druse (d); intercapillary pillars (black arrowheads) between CC lumens (asterisks); BrM over CC lumens (white arrowheads, called non-pillar areas in wholemount perspective). (**C**) Sample from a similar region after RPE and sub-RPE debris is completely removed. BrM is intact, and symbols correlate with descriptions in **B**. Bar = 10 μm.

and decreases the vital exchange between the RPE and the choriocapillaris (Ethier et al. 2004). It is thought that this process causes metabolic stress, impairs retinal function, and contributes with other environmental and genetic factors to the onset of age-related macular degeneration (ARMD), a major cause of vision loss in the elderly (Zarbin 1998; Beatty et al. 2000; Hageman et al. 2005; Edwards and Malek 2007). Lipid accumulation in human BrM also contributes to the formation of drusen (for druse example, see Figure 1B) and basal linear deposits, ARMD-associated extracellular lesions between the RPE basal lamina and BrM.

BrM in the macula accumulates more lipids and is more vulnerable to disease progression than the peripheral retina. Direct assays of lipid composition, although possible (Holz et al. 1994; Curcio et al. 2001; Wang et al. 2009), are difficult, in part due to the challenge of cleanly isolating BrM from the underlying choroid. We thought that mapping the detailed deposition of lipids in BrM wholemounts would provide an informative perspective. Maps are advantageous because they provide an en face view familiar from clinical ophthalmology. Further, they can be compared with the topography of other chorioretinal features such as photoreceptors and the BrM elastic layer (Curcio et al. 1990; Chong et al. 2005), with the hope that similar topographies will indicate mechanistically related processes. Finally, wholemounts stained with fluorescent dyes specific for lipids permit semiquantitative evaluation (Rudolf et al. 2007).

For a study of BrM lipid topography, we sought a wholemount preparation that provided largely intact BrM, maximal flatness of BrM to permit good focus, and a thin choroid to facilitate dye penetration. To optimize tissue contrast, we sought a means to label BrM with little interference from either stain or autofluorescence elsewhere in the choroid.

Because published wholemount methods did not meet our specific requirements (McMenamin 2000), we developed a BrM preparation with a thin choroid, and we tested several fluorescent neutral lipid stains.

We used Oil Red O, the best-known member of the Red Sudan family (Adams and Bayliss 1975), Nile Red, a red phenoxazone dye (Greenspan et al. 1985), BODIPY 493/503, a non-polar derivate of the BODIPY fluophore, and filipin, a polyene antibiotic (Norman et al. 1972; Kruth et al. 1987). Oil Red O, Nile Red, and BODIPY 493/503 are lysochromes, i.e., they partition directly into hydrophobic lipids. In contrast, filipin binds specifically to sterols, interacting with the 3β-hydroxy group of cholesterol. In EC, this site is esterified to a fatty acid and has to be hydrolyzed first with cholesterol esterase to release filipin-accessible cholesterol. We anticipated different staining patterns with each dye, because they recognize different lipid classes (Table 1). These data can help us interpret the conflicting conclusions of studies deducing

Table 1 Dye specificities

	Oil Red O	Nile Red	BODIPY 493/503[a]	Filipin
FFA	+	+	+	−
TG	+	+	+	−
UC	−	+	+	+
EC	+	+	+	−[b]
PL	−	(+)	−	−
Fluo-intensity	(+)	+++	++	++

[a]Presumed specificities due to the resemblance of sections to Nile Red–stained sections.
[b]To demonstrate EC with filipin, UC has to be extracted with 70% ethanol and the remaining EC converted by cholesterol esterase into filipin-detectable UC. Fluorescence intensity was indirectly evaluated by comparing exposure times required to achieve comparably bright fluorescent images in chorioretinal sections with otherwise constant conditions. +++, strong; ++, medium; +, low; (+), very low; −, none.
Dye specificities according to published studies (Bittman and Fischkoff 1972; Adams and Bayliss 1975; Greenspan et al. 1985; Kruth et al. 1987; Gocze and Freeman 1994; Koopman et al. 2001; Sheu et al. 2003). Neutral lipids: free fatty acids (FFA), triglyceride (TG), unesterified cholesterol (UC), esterified cholesterol (EC); polar lipids: phospholipids (PL). +, reliably detected; (+), variably detected; −, not detected.

sources of these lipids from direct assay of the BrM–choroid complex (Holz et al. 1994; Curcio et al. 2001).

Herein, we describe an improved wholemount preparation that emphasizes flatness of the BrM side of the choroid. We describe new staining patterns in BrM wholemounts and compare them to patterns in vertical cross sections through the retina and choroid.

Materials and Methods

Institutional Review at the University of Alabama at Birmingham approved our use of human tissues. From the Alabama Eye Bank, we obtained eyes from 16 Caucasian donors (ages 65–93 years) with no grossly visible drusen or pigmentary changes in the macula.

Tissue Processing

Eyes were preserved by immersion in either 4% paraformaldehyde or 1% paraformaldehyde/2.5% glutaraldehyde, both in 0.1 M phosphate buffer, for 24 hr following removal of the anterior segment, and then stored in 1% paraformaldehyde at 4C until used. Median time between death and preservation was 5.7 hr. Tissue was processed either for chorioretinal sections or BrM–choroid wholemounts.

For chorioretinal sections, 7 × 7-mm-wide samples from 6 eyes, containing retina, RPE, and choroid, were cut from the posterior pole with a razor blade. Samples were cryo-protected by infiltration with successive solutions of 10%, 20%, and 30% sucrose in phosphate buffer, 4:1 30% sucrose-OCT (Histoprep; Fisher Scientific, Pittsburgh PA) solution, and 2:1 30% sucrose-OCT solution for 30 min each, and then frozen in liquid nitrogen. Specimens were sectioned at 10 μm (CM3000 cryostat; Leica Microsystems Inc., Bannockburn, IL). Consecutive sections were collected on gelatin-subbed slides, air-dried for 4 hr, and stored at −20C until further use.

For BrM–choroid wholemounts, globes of 10 eyes were incised circularly posterior to the vitreous base (Figure 1), so that the anterior segment, including the vitreous body, could be removed together. All further tissue preparation was done under stereomicroscopic control (SMZ-U; Nikon Instruments, Inc., Melville, NY). The remaining retina (Figure 2A) was easily detached and could be separated from the optic nerve head with an ophthalmic crescent knife (Alcon Laboratories; Ft. Worth, TX). Tissue was kept moist with PBS. RPE (on in Figure 2B, off in Figure 2C) was either

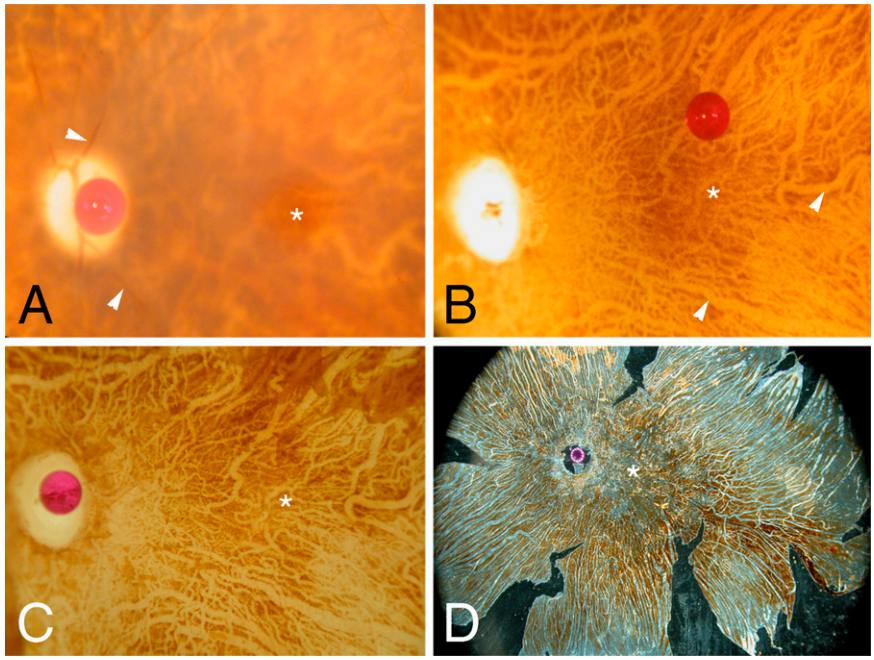

Figure 2 Wholemount preparation of one donor eye. Asterisk, fovea; optic nerve head is marked by a red scale bead (diameter = 1 mm) in **A,C,D**. (**A**) Postmortem central fundus. The retina is blurred with thinned retinal vessels (arrowheads); only the fovea is still transparent. (**B**) Neuroretina removed. Large choroidal vessels, devoid of blood, appear as lighter lines (arrowheads) in the background. (**C**) Fundus during RPE removal. Upper-right corner, remaining RPE; choroidal vessels clearly visible. (**D**) Transillumination of a complete wholemount after removal of all large choroidal vessels, leaving a transparent negative of the vascular network; only choriocapillaris and pigmented connective tissue is left, mounted on a silane coverslip for air-drying. After drying and staining, the coverslip has to be flipped into final position for examination under the microscope.

brushed off with a fine round art brush (Taklon Loew-Cornell, Inc.; Englewood Cliffs, NJ), wiped off with a blunt spatula, or if the preparation was difficult due to fixation, gently scraped off with a rounded surgical blade (no. 57; Alcon Laboratories). The remaining BrM–choroid complex was dissected into nine pie-like wedges. Wedges were easily separated from the sclera with the crescent knife by lifting the tissue and cutting the large choroidal vessels parallel to the sclera with small circular movements. The optic nerve head was also removed with the crescent knife. With the wedges facing BrM down, choroidal vessels and connective tissue were removed with fine-tip tweezers (WPI; Sarasota, FL) and art brushes. The tissue was further processed for staining. In a concurrent study, we successfully used this mounting technique on six complete wholemounts (Figure 2D) (Rudolf et al. 2007). To monitor the completeness of choroidal removal, we collected 2 × 2–mm samples at random for resin embedding. Samples were dehydrated using ethanol and propylene oxide and were embedded in epoxy resin (PolyBed 812; Polysciences, Warrington, PA). Blocks were sectioned serially at 1 μm (Ultracut UCT; Leica Mikrosysteme AG, Vienna, Austria), stained with 1% toluidine-O blue, and coverslipped for evaluation by light microscopy.

Optimal flatness on the BrM side of the tissue was crucial for reliable and repeatable results in fluorescence microscopy. We maximized flatness by mounting the tissue on organosilane-pretreated coverslips (not slides) with BrM facing the glass surface. The organosilane pretreatment guaranteed better tissue adherence to the coverslips and constant alignment of BrM with the glass surface. We pretreated the coverslips manually as follows. After an acetone wash, they were exposed for 1 min to 4% 3-aminopropyltriethoxy-silane (Sigma Chemical Co.; St. Louis, MO) in acetone, rinsed again with acetone, and air-dried (Hayat 2002). The choroid was carefully oriented on coverslips under stereoscopic control and arranged flat and wrinkle-free. Excessive fluid was absorbed with surgical wedge sponges, and specimens were air-dried overnight. The wholemounts stayed securely attached to the coverslips through the following procedures.

Staining for Chorioretinal Sections

Slides with sections were removed from the freezer, air-dried for 1 hr, rehydrated for 15 min with PBS, and stained as described below. All stains were directly applied to slides for 1 hr in a light-blocking box. Slides were rinsed four times with PBS and coverslipped with Glycergel (DAKO; Glostrup, Denmark). Light exposure was minimized during handling. We employed four stains: (1) Oil Red O (6 mg/ml; Sigma) in 60% triethyl phosphate, diluted with distilled water to 3 mg/ml, and filtered (Whatman filter no. 42; Whatman, Piscataway, NJ) (Koopman et al. 2001); (2) Nile Red (0.5 mg/ml in acetone; Sigma), diluted with PBS to 1.75 μg/ml; (3) BODIPY 493/503 (0.5 mg/ml; Molecular Probes, Inc., Eugene, OR) in 100% ethanol, diluted with PBS to 20 μg/ml; (4) filipin for unesterified cholesterol (UC-F), dissolved in *N*,*N*-dimethyl formamide (2.5 mg/ml; Sigma), diluted with PBS to 250 μg/ml; and (5) filipin for esterified cholesterol (EC-F), which required two additional steps prior to staining, as follows. UC was extracted with 70% ethanol for 30 min, and the remaining EC was hydrolyzed by cholesterol esterase (15 μg/ml; Roche Diagnostics, Indianapolis, IN) in 0.1 M potassium phosphate buffer, pH 7.4, at 37C for 3.5 hr (Kruth et al. 1987; Curcio et al. 2001,2005). The product of this reaction was newly released UC, which was recognizable by filipin (Kruth et al. 1987).

Staining of Wholemounts

All tissues mounted BrM down on coverslips were rehydrated with PBS for 10 min and treated with proteinase K (1 μg/ml, Sigma, in PBS) for 15 min. Filipin (500 μg/ml), Oil Red O (6 mg/ml), Nile Red (3.5 μg/ml), and BODIPY 493/503 (40 μg/ml) were applied to the specimens for 2.5 hr, followed by five rinses with PBS. Light exposure was minimized. Coverslips were inverted and mounted on glass micro slides with Glycergel. BrM was now facing up for microscopy, still aligned to the coverslip's counterface. A pretreatment was necessary for EC-F. For uniform results, wholemounts were exposed to the following solutions free-floating on a slowly moving shaker table. After 10 min in proteinase K (1 μg/ml) in PBS and three rinses with PBS, UC was extracted by 70% ethanol for 1 hr, followed by five rinses with PBS, and hydrolysis of EC by cholesterol esterase (30 μg/ml; Roche Diagnostics) for 5 hr at 37C. Released UC was detectable again by filipin.

Control Experiments

Additionally, we performed several control experiments for both chorioretinal sections and wholemounts (Curcio et al. 2001,2005). First, untreated tissue was viewed with different fluorescent filter sets to reveal autofluorescence. Second, we completely extracted all lipids with Folch's reagent (chloroform-methanol 2:1) before applying the different lipid stains. Third, for EC-F, after ethanol extraction, no cholesterol esterase was applied before filipin staining.

Evaluation

Chorioretinal sections and BrM–choroid wholemounts were examined using differential interference contrast (DIC) microscopy (Eclipse 80i; Nikon Instruments, Inc., Melville, NY) and 20×, 40×, and 60× (oil immersion)

planapochromat objectives. Images were captured using a digital camera (Retiga 4000R Fast; QImaging, Burnaby, BC, Canada) and the accompanying software (Qcapture v2.8.1; QImaging). Corresponding images were taken in wide-field epi-fluorescence mode. The following filter cubes (Chroma Technology Corp.; Rockingham, VT) were used: for filipin UV-2A, excitation 350/50, emission 420 long-pass; for BODIPY 493/503 B-2E/C, excitation 480/30, emission 535/40; for Oil Red O, excitation 560/20 and Nile Red G-3E/C, excitation 540/25, emission 605/55.

Results

Preparation Quality of BrM–Choroid Wholemounts

Light microscopy of 1-μm sections of random samples showed thin BrM–choroid wholemounts with a thickness of 27–47 μm (Figure 1C), compared with a native choroid thickness of 160–300 μm (Holz et al. 2004). The RPE and sub-RPE deposits like drusen (Figures 2A–2D) were completely removed in the macula and mid-periphery. Occasionally, small patches of remaining RPE cells and drusen remained attached to BrM in areas from near the vitreous base, anterior to the ocular equator. RPE and drusen were much more adherent there, and not removing these small islands was a fair tradeoff for maintaining BrM integrity. On the other side of the tissue, removal of all larger choroidal vessels and choroidal connective tissue was manageable; but overall, it was a time-consuming (8 hr) and delicate task.

Staining Controls

Control experiments confirmed that the fluorescence signal after staining was specific and attributable to the presence of lipids and dye characteristics. All control experiments showed negative results. A minimum autofluorescence was visible with the ultraviolet filter in BrM/choroid of all specimens (Figures 3H and 4H). The RPE accumulates strongly fluorescent lipofuscin with age, and the broadband excitation and emission of lipofuscin and its major fluorophor, A2E (Marmorstein et al. 2002), interfered with all fluorescent filter sets (Figure 3). We removed the RPE from the wholemounts but it was retained in the sections. Complete lipid extraction before staining confirmed the specificity of dyes for lipids, because no signal higher than the natural autofluorescence of the tissue was apparent (not shown). Only Nile Red demonstrated some moderate spotty hyperfluorescence in a few extracted samples. The staining procedure for EC-F involved UC extraction followed by a hydrolysis of EC to filipin-detectable UC by cholesterol esterase. Skipping the hydrolysis step showed a negative result and confirmed the specificity of this method for EC (not shown).

Staining Intensity

We used the exposure times required for achieving comparably bright fluorescent images in chorioretinal sections (with otherwise constant conditions) as surrogates for the fluorescent intensities of the different stains. Nile Red was by far the most strongly fluorescing dye. BODIPY 493/503 and filipin both demonstrated strong overall fluorescence (Table 2). Oil Red O fluorescence intensity was the weakest of our tested dyes (Table 2), but the intensity was still higher than BrM autofluorescence with the same filters and camera settings.

Staining Pattern

For chorioretinal sections (Table 2), Figure 3A (DIC) and Figure 3B (Oil Red O, bright-field) depict the layered anatomy of the chorioretinal specimens. BrM stained intensely with Oil Red O, including the intercapillary pillars (Figure 1) and, occasionally, the walls of a few choroidal arteries (Figure 3B). Photoreceptor outer segments occasionally exhibited a faint dull red. Other structures were negative. Figure 3C shows Oil Red O weak fluorescence in the same locations, with a moderate background signal. In comparison, Nile Red, BODIPY 493/503, and UC-F stained retina and choroid, but always showed their highest intensity on the level of BrM (Figures 3D–3F). EC-F was specific for BrM and occasionally the intima of larger choroidal arteries, but all other structures were negative (Figure 3G). With all dyes, BrM always presented as a continuous band with high fluorescence intensity.

For BrM–choroid wholemounts, we found an overall good penetration of reagents, as indicated by evenly distributed fluorescence intensity across the sample and no highlighting of the tissue's borders relative to its center. When viewed with DIC microscopy, little anatomical detail was apparent in the BrM wholemount (Figure 4A). Oil Red O revealed in bright-field microscopy light-red staining of the entire BrM accented by more strongly stained intercapillary pillars (Figure 4B), especially around their borders. Oil Red O fluorescence was very weak (Figure 4C) and barely different from autofluorescence (Figure 4H). In contrast, Nile Red (Figure 4D) and BODIPY 493/503 (Figure 4E) demonstrated an overall strong fluorescence from intercapillary pillars and BrM non-pillar areas. Intercapillary pillars were often more intense but also regularly cross-faded with BrM non-pillar areas and deeper choroidal structures so that digital adjustments in contrast and brightness were required to enhance pillar visibility. UC-F staining demonstrated no distinct pattern (Figure 4F). The appearance was blurry overall, and fluorescence seemed to derive from unfocusable structures within the tissue.

In general, EC-F stained BrM very well and was not notably blocked by other structures (Figure 4G). Only EC-F–positive material was highly localized to BrM

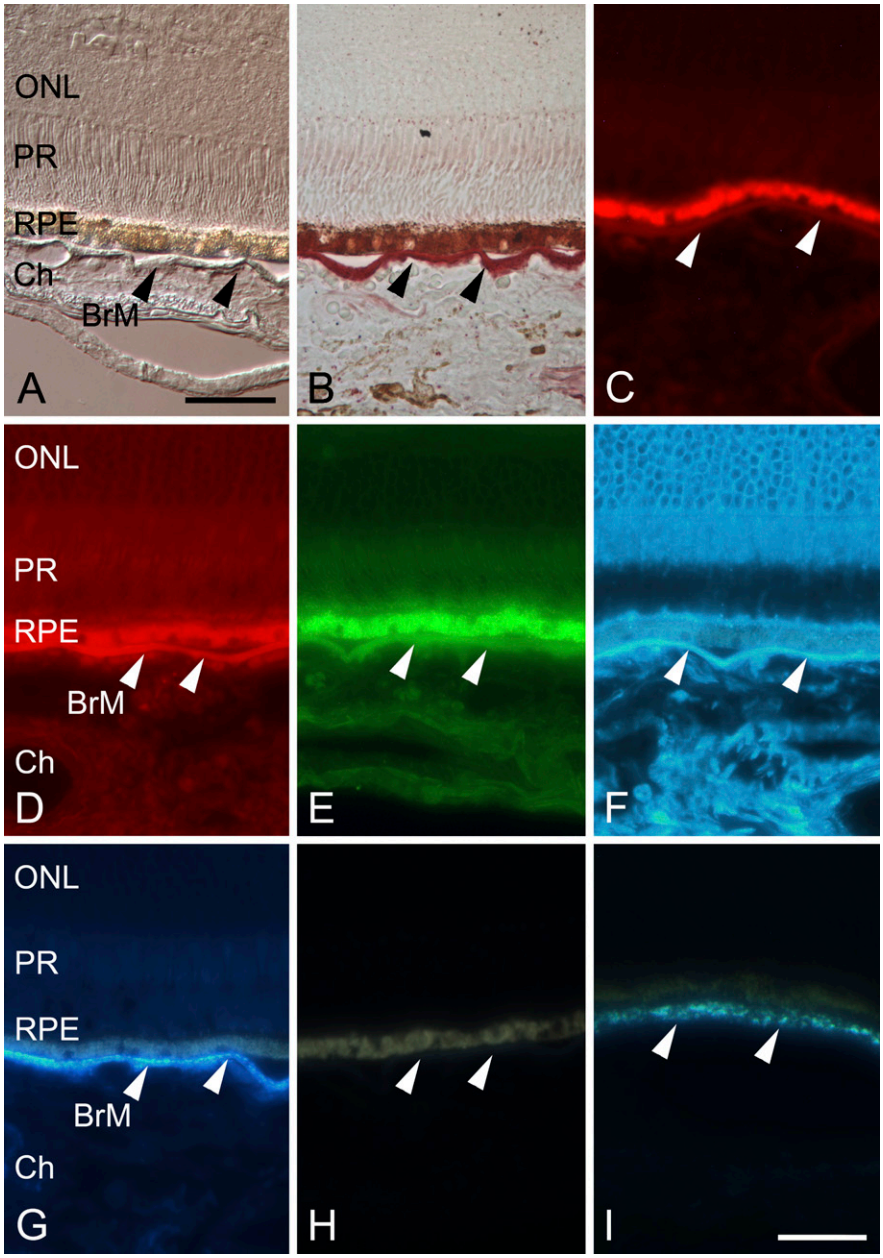

Figure 3 Neutral lipid stains in sections of retina and choroid. Arrowheads indicate BrM. The RPE is strongly autofluorescent over all investigated spectra, owing to age-related accumulation of lipofuscin. ONL, retina's outer nuclear layer; PR, photoreceptors; Ch, choroid. (**A**) Unstained section viewed with differential interference contrast (DIC). (**B**) Section stained with Oil Red O and viewed with bright-field microscopy demonstrates strong red coloration of BrM, including the intercapillary pillars. BrM is slightly detached from the RPE and bowed downward in three locations. (**C**) Wide-field epifluorescence showing only a very weak fluorescence of Oil Red O. (**D**) Section stained with Nile Red, demonstrating strong (main) signal in BrM and staining in other structures in Ch and retina as well (strong background signals). The same applies to the BODIPY 493/503–stained section shown in **E**. (**F**) Unesterified cholesterol (UC) stained with filipin demonstrated a strong reaction in retina, BrM, and Ch. (**G**) Isolated signal in BrM found for esterified cholesterol (EC) after pretreatment (see Methods) stained with filipin. (**H**) Unstained section demonstrating the tissue autofluorescence imaged with the same ultraviolet (UV) filter and image-capture settings as shown in **F** and **G**. (**I**) At higher magnification, EC-F in peripheral section has a granular appearance. Bars: **A** = 50 μm for **A–H**; **I** = 20 μm.

and revealed reproducible and distinctive distribution patterns. In general, the intercapillary pillars were more intensely stained than the adjacent non-pillar areas. Staining revealed a highly specific granular staining pattern. With this knowledge, we looked again at chorioretinal sections and found a comparable granular pattern in the periphery with the 60× objective only (Figure 3I), when exposure times were reduced.

Discussion

Age-related accumulation of neutral lipids in BrM is a major part of the underlying biology of ARMD, yet its analysis with valid and reliable methods is technically challenging. Here we solve several problems to characterize BrM lipid topography and compare it to other chorioretinal features. BrM is a delicate layer just 2–4 μm thick on one side of a large vascular tissue that is not particularly flat. We wished to achieve an intact and evenly stained tissue, a constant maximum flatness at the level of BrM, a distinctive and recognizable staining pattern, and a fluorescent marker that lent itself to semiquantitative evaluation. We found that mounting and air-drying wholemounts of the partially stripped choroid with the BrM side up on organosilane-pretreated coverslips, before staining, produced optimal

The Journal of Histochemistry & Cytochemistry

Table 2 Staining results in chorioretinal sections

	Oil Red O	Nile Red	BODIPY 493/503	UC-F	EC-F
Retina	−	+++	++	++	−
BrM	++	+++	++	++	++
Choroid	+	+++	++	++	−

BrM, Bruch's membrane; UC-F, filipin for unesterified cholesterol; EC-F, filipin for esterified cholesterol. Intensity of fluorescent staining: +++, strong; ++, medium; +, low; −, none. Large vasculature, identified within the retina and choroid in light microscopy with deferential interference contrast, was not included the evaluation of the above-mentioned structures.

tissue flatness for microscopy. We assessed different fluorescent lipid dyes and found that filipin following cholesterol esterase treatment was most informative.

As previously described, we localized EC almost exclusively to BrM, with additional staining in an occasional arterial intima in the choroid (Kruth 1997; Curcio et al. 2001). However, the wholemounts revealed staining patterns not previously appreciated in chorioretinal sections. In particular, we noted an intense and very distinct granular pattern for EC-F. With this new knowledge, higher magnification, and optimal exposure, we then detected a similar pattern in peripheral BrM, where the EC concentration is lower (Curcio et al. 2001; Rudolf et al. 2007). We suspected that the granules may represent single or clustered EC-rich lipoprotein particles 60–80–nm in diameter that are isolable from BrM (see below) (Li et al. 2005b; Wang et al. 2009). The wholemount perspective also highlighted the intercapillary pillars as areas of intense lipid deposition that might further impede transport across BrM. The pathogenic significance of intercapillary pillars is shown by their association with drusen in the peripheral retina of virtually every aged eye (Lengyel et al. 2004).

Characteristics of different dyes and their selectivity for different classes provide information valuable for interpreting BrM lipid composition data. In chorioretinal sections, all dyes stained BrM most intensely, due to high EC concentration. In contrast, weak polar UC and polar phospholipids are common elements of all cellular and intracellular membranes and are therefore ubiquitous across tissue sections. Filipin, which binds to the 3β-hydroxy group of sterols (Norman et al. 1972), proved best for our purposes. It was highly specific for both UC and EC. Staining of untreated tissue demonstrated abundant UC in retina, BrM, and choroid. Following UC extraction with ethanol and hydrolysis, filipin localized exclusively to BrM. Despite its evident utility, filipin is not ideal, inasmuch as it faded with time and was not sufficiently robust for laser confocal

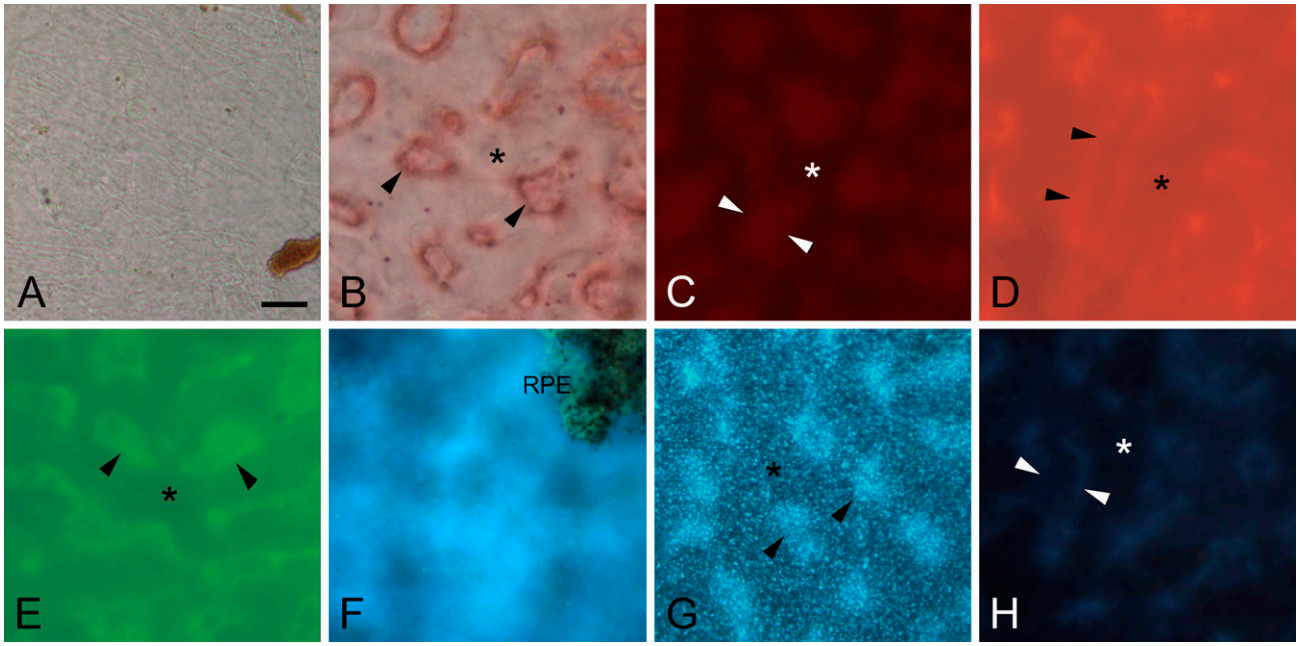

Figure 4 Neutral lipid stains in BrM wholemounts. Outer macula, RPE removed. Arrowheads, intercapillary pillars of BrM; asterisk, BrM over choriocapillaris. (**A**) In unstained section viewed with DIC, intercapillary pillars were hardly visible. Shown in lower right is remaining choroidal pigment. (**B**) Section stained with Oil Red O viewed with bright-field microscopy with light-red coloration of BrM and intense outlining of the intercapillary pillars. (**C**) In dark-field mode, weak fluorescence of Oil Red O of intercapillary pillars only. Wholemounts stained with Nile Red (**D**) and BODIPY 493/503 (**E**) show comparable patterns, with strong background fluorescence from the choroid. Intercapillary pillars are visible only if images are regularly enhanced by image-processing software (contrast/brightness). (**F**) UC stained with filipin. Upper right, an island of RPE was left for better orientation. Weak, inconsistent signal from BrM, major interference by choroidal connective tissue background. (**G**) EC: filipin regularly stained a granular pattern with increased intensity in intercapillary pillars. (**H**) Wholemount preparation imaged with same filter (UV) and image-capture settings as in **F** and **G**. Bar = 40 μm.

The Journal of Histochemistry & Cytochemistry

microscopy. Nevertheless, our topography study in progress used only filipin staining.

Oil Red O is the classic neutral lipid stain best analyzed in bright-field microscopy. It penetrates highly hydrophobic lipid droplets that contain free fatty acids, triglycerides, and EC (Table 1) but not lipids with some polar properties, like UC and phospholipids (Adams and Bayliss 1975). In chorioretinal sections and wholemounts, it labels almost exclusively BrM, and indeed this technique was used for the initial description of lipids in aged BrM (Pauleikhoff et al. 1990). Even though this degree of specificity is highly desirable, we could not replicate the specific fluorescent label ing reported elsewhere (Koopman et al. 2001), and therefore Oil Red O was less useful to us as a quantifiable fluorophor.

Nile Red and BODIPY 493/503 are both strongly fluorescent and reveal a broader range of lipids than does Oil Red O, including UC. Nile Red has a broad fluorescence spectrum from yellow to red, depending on the relative hydrophobicity of the mixed lipids. Around non-polar triglycerides and EC, Nile Red fluoresces yellow-golden, and around polar phospholipids, red (Greenspan and Fowler 1985). Our results indicate that predominantly, structures rich in phospholipids were stained. Nile Red also highlights proteins with hydrophobic domains (Greenspan and Fowler 1985), perhaps explaining the spotty fluorescence in control tissues after ostensibly complete lipid extraction. BODIPY 493/503, a non-polar derivate (difluoropentamethyl-bora-diaza-*s*-indacene) of the BODIPY fluophore (difluoro-diaza-*s*-indacene) is somewhat more specific for intracellular lipid droplets, presumably not staining phospholipids such as Nile Red (Table 1) (Greenspan and Fowler 1985; Gocze and Freeman 1994). In our hands, Nile Red and BODIPY 493/503 stained structures throughout chorioretinal sections and wholemounts, causing strong background signals and hindering sharp focus.

Our improved methods for studying BrM lipids are noteworthy because age is the largest risk factor for ARMD, and the accumulation of neutral lipids in BrM is one of the largest and least-understood age changes in human retina. Direct assay has validated both the presence of EC in BrM and its predominance over other lipid classes in the same tissue (Curcio et al. 2001; Haimovici et al. 2001; Li et al. 2005b; Wang et al. 2009). EC, the most-hydrophobic neutral lipid, is the cholesterol form used for intra-cellular storage and for transport through plasma within the neutral lipid cores of lipoprotein particles. Strong ultrastructural evidence indicates that lipoprotein-like particles localize to BrM and to sub-RPE deposits (Curcio et al. 2005; Huang et al. 2007,2008). Further, lipoprotein-like particles containing abundant EC and apolipoproteins B, A-I, and E are isolable from BrM (Li et al. 2005a; Wang et al. 2009). Finally, the RPE expresses a functional pathway for the synthesis, assembly, and secretion of large EC-rich, apolipoprotein B–containing particles (Li et al. 2005b; Wang et al. 2009). Therefore, RPE is a plausible source, and lipoprotein particles a plausible mechanism, to explain the histochemically prominent EC in BrM. We expect that quantifying the topography of this material will provide insights into the function of this unusual process within the eye.

In conclusion, we developed a BrM–choroid wholemounting technique suitable for reliable staining and evaluation. No dye provided perfect characteristics in regard to representing all neutral lipids or to fluorescence intensity, but we found only EC, visualized by filipin, highly localized to BrM with a specific granular pattern. Because we know by direct assay that EC is abundantly present in BrM, we consider EC-F the most valuable choice for analyzing neutral lipid deposits in human BrM.

Acknowledgments

This project was supported by the Macula Vision Research Foundation, Deutsche Forschungsgemeinschaft (DFG 13942), and Research to Prevent Blindness.

We thank Susan Vogt, M.Sc., and Melissa Chimento, B.Sc., for technical assistance. We also thank the Alabama Eye Bank for timely retrieval of donor eyes.

Literature Cited

Adams CWM, Bayliss OB (1975) Lipid histochemistry. In Glick D, Rosenbaum RM, eds. Techniques of Biochemical and Biophysical Morphology. 2nd ed. New York, John Wiley and Sons, 100–156

Beatty S, Koh H, Phil M, Henson D, Boulton M (2000) The role of oxidative stress in the pathogenesis of age-related macular degeneration. Surv Ophthalmol 45:115–134

Bittman R, Fischkoff SA (1972) Fluorescence studies of the binding of the polyene antibiotics filipin 3, amphotericin B, nystatin, and lagosin to cholesterol. Proc Natl Acad Sci USA 69:3795–3799

Chong NH, Keonin J, Luthert PJ, Frennesson CI, Weingeist DM, Wolf RL, Mullins RF, et al. (2005) Decreased thickness and integrity of the macular elastic layer of Bruch's membrane correspond to the distribution of lesions associated with age-related macular degeneration. Am J Pathol 166:241–251

Curcio CA, Millican CL, Bailey T, Kruth HS (2001) Accumulation of cholesterol with age in human Bruch's membrane. Invest Ophthalmol Vis Sci 42:265–274

Curcio CA, Presley JB, Malek G, Medeiros NE, Avery DV, Kruth HS (2005) Esterified and unesterified cholesterol in drusen and basal deposits of eyes with age-related maculopathy. Exp Eye Res 81:731–741

Curcio CA, Sloan KR, Kalina RE, Hendrickson AE (1990) Human photoreceptor topography. J Comp Neurol 292:497–523

Edwards AO, Malek G (2007) Molecular genetics of AMD and current animal models. Angiogenesis 10:119–132

Ethier CR, Johnson M, Ruberti J (2004) Ocular biomechanics and biotransport. Annu Rev Biomed Eng 6:249–273

Gocze PM, Freeman DA (1994) Factors underlying the variability of lipid droplet fluorescence in MA-10 Leydig tumor cells. Cytometry 17:151–158

Greenspan P, Fowler SD (1985) Spectrofluorometric studies of the lipid probe, nile red. J Lipid Res 26:781–789

Greenspan P, Mayer EP, Fowler SD (1985) Nile red: a selective fluorescent stain for intracellular lipid droplets. J Cell Biol 100:965–973

Hageman GS, Anderson DH, Johnson LV, Hancox LS, Taiber AJ, Hardisty LI, Hageman JL, et al. (2005) A common haplotype in the complement regulatory gene factor H (HF1/CFH) predisposes individuals to age-related macular degeneration. Proc Natl Acad Sci USA 102:7227–7232

Haimovici R, Gantz DL, Rumelt S, Freddo TF, Small DM (2001) The lipid composition of drusen, Bruch's membrane, and sclera by hot stage polarizing light microscopy. Invest Ophthalmol Vis Sci 42:1592–1599

Hayat MA (2002) Microscopy, Immunohistochemistry, and Antigen Retrieval Methods: For Light and Electron Microscopy. 1st ed. New York, Springer, 68

Hogan MJ (1972) Role of the retinal pigment epithelium in macular disease. Trans Am Acad Ophthalmol Otolaryngol 76:64–80

Holz FG, Schuett F, Pauleikhoff D, Bird AC (2004) AMD pathophysiology. In Holz FG, Pauleikhoff D, Spaide RF, Bird AC, eds. Age-related Macula Degeneration. Berlin, Heidelberg, Springer-Verlag, 32–46

Holz FG, Sheraidah G, Pauleikhoff D, Bird AC (1994) Analysis of lipid deposits extracted from human macular and peripheral Bruch's membrane. Arch Ophthalmol 112:402–406

Huang JD, Curcio CA, Johnson M (2008) Morphometric analysis of lipoprotein-like particle accumulation in aging human macular Bruch's membrane. Invest Ophthalmol Vis Sci 49:2721–2727

Huang JD, Presley JB, Chimento MF, Curcio CA, Johnson M (2007) Age-related changes in human macular Bruch's membrane as seen by quick-freeze/deep-etch. Exp Eye Res 85:202–218

Koopman R, Schaart G, Hesselink MK (2001) Optimisation of oil red O staining permits combination with immunofluorescence and automated quantification of lipids. Histochem Cell Biol 116:63–68

Kruth HS (1997) The fate of lipoprotein cholesterol entering the arterial wall. Curr Opin Lipidol 8:246–252

Kruth HS, Cupp JE, Khan MA (1987) Method for detection and isolation of cholesteryl ester-containing "foam" cells using flow cytometry. Cytometry 8:146–152

Lengyel I, Tufail A, Hosaini HA, Luthert P, Bird AC, Jeffery G (2004) Association of drusen deposition with choroidal intercapillary pillars in the aging human eye. Invest Ophthalmol Vis Sci 45:2886–2892

Li CM, Chung BH, Presley JB, Malek G, Zhang X, Dashti N, Li L, et al. (2005a) Lipoprotein-like particles and cholesteryl esters in human Bruch's membrane: initial characterization. Invest Ophthalmol Vis Sci 46:2576–2586

Li CM, Presley JB, Zhang X, Dashti N, Chung BH, Medeiros NE, Guidry C, et al. (2005b) Retina expresses microsomal triglyceride transfer protein: implications for age-related maculopathy. J Lipid Res 46:628–640

Marmorstein AD, Marmorstein LY, Sakaguchi H, Hollyfield JG (2002) Spectral profiling of autofluorescence associated with lipofuscin, Bruch's Membrane, and sub-RPE deposits in normal and AMD eyes. Invest Ophthalmol Vis Sci 43:2435–2441

McMenamin PG (2000) Optimal methods for preparation and immunostaining of iris, ciliary body, and choroidal wholemounts. Invest Ophthalmol Vis Sci 41:3043–3048

Norman AW, Demel RA, de Kruyff B, van Deenen LL (1972) Studies on the biological properties of polyene antibiotics. Evidence for the direct interaction of filipin with cholesterol. J Biol Chem 247:1918–1929

Pauleikhoff D, Harper CA, Marshall J, Bird AC (1990) Aging changes in Bruch's membrane. A histochemical and morphologic study. Ophthalmology 97:171–178

Rudolf M, Li CM, Chimento MF, Curcio CA (2007) Topography of esterified cholesterol deposition in human Bruch membrane wholemounts. Invest Ophthalmol Vis Sci 48:2184

Sheu HM, Tsai JC, Lin TK, Wong TW, Lee JY (2003) Modified Nile red staining method for improved visualization of neutral lipid depositions in stratum corneum. J Formos Med Assoc 102: 656–660

Wang L, Li CM, Rudolf M, Belyaeva OV, Chung BH, Messinger JD, Kedishvili NY, et al. (2009) Lipoprotein particles of intraocular origin in human Bruch membrane: an unusual lipid profile. Invest Ophthalmol Vis Sci 50:870–877

Zarbin MA (1998) Age-related macular degeneration: review of pathogenesis. Eur J Ophthalmol 8:199–206

The Journal of Histochemistry & Cytochemistry